Popular Summary of "Extratropical Stratosphere-Troposphere Mass Exchange"

Mark Schoeberl

Understanding the exchange of gases between the stratosphere and the troposphere is important for determining how pollutants enter the stratosphere and how they leave. This study does a global analysis of that the exchange of mass between the stratosphere and the troposphere. While the exchange of mass is not the same as the exchange of constituents, you can't get the constituent exchange right if you have the mass exchange wrong. Thus this kind of calculation is an important test for models which also compute trace gas transport.

In this study I computed the mass exchange for two assimilated data sets and a GCM. The models all agree that amount of mass descending from the stratosphere to the troposphere in the Northern Hemisphere extra tropics is $\sim 10^{10}$ kg/s averaged over a year. The value for the Southern Hemisphere by about a factor of two. (10^{10} kg of air is the amount of air in 100 km x 100 km area with a depth of 100 m – roughly the size of the D.C. metro area to a depth of 300 feet.)

Most people have the idea that most of the mass enters the stratosphere through the tropics. But this study shows that almost 5 times more mass enters the stratosphere through the extra-tropics. This mass, however, is quickly recycled out again. Thus the lower most stratosphere is a mixture of upper stratospheric air and tropospheric air. This is an important result for understanding the chemistry of the lower stratosphere.

Extratropical Stratosphere-Troposphere Mass Exchange

Mark R. Schoeberl
Earth Sciences Directorate
NASA Goddard Space Flight Center
Greenbelt, Md.

Abstract

The net mass flux from the stratosphere to the troposphere can be computed from the heating rate along the 380K isentropic surface and the time rate of change of the mass of the lowermost stratosphere (the region between the tropopause and the 380K isentrope). Given this net mass flux and the cross tropopause diabatic mass flux, the residual adiabatic mass flux across the tropopause can also be estimated. These fluxes have been computed using meteorological fields from a free-running general circulation model (FVGCM) and two assimilated data sets, FVDAS, and UKMO. All of the calculations agree that the annual average net mass flux for the Northern Hemisphere is about 10^{10} kg/s. There is less agreement on the Southern Hemisphere flux that might be half as large. For all three data sets, the adiabatic mass flux is from the upper troposphere into the lowermost stratosphere. This adiabatic flux into the lowermost stratosphere is up to five times larger than the diabatic mass flux into the stratosphere across the tropical tropopause. For the FVDAS, the mid-latitude tropopause diabatic flux is smaller than UKMO apparently due to a systematically colder, higher FVDAS tropopause. Both data assimilation systems have a warmer, lower mid-latitude tropopause compared to radiosondes so the mass flux estimates can be considered upper bounds, Finally, we note that the difference in the diabatic mass fluxes between the two assimilated meteorological analyses is much larger than the interannual variability in either.

1. Introduction

One of the more difficult problems in dynamic meteorology is the determination of the amount of mass exchanged between the stratosphere and the troposphere. This problem

is important since the exchange rate between the stratosphere and the troposphere is directly related to the residence time of stratospheric trace constituents that are linked to ozone destruction. The stratosphere is also a significant source for tropospheric ozone, on the order of 500 Tg/year [Olsen et al. 2002, and references therein].

It is now common knowledge that air primarily enters the stratosphere in the tropics and sinks back into the troposphere at extratropical latitudes as part of the Brewer-Dobson circulation [Brewer, 1949; Dobson, 1956; Holton et al., 1995]. The mid-latitude downward flux across the extratropical tropopause has a seasonal component that was first revealed by the radioactive tracers studied by Staley [1962], and stratosphere-troposphere exchange (STE) is often accompanied by spectacular cyclogenesis [Danielsen, 1968; Shapiro, 1980, Appenzeller and Davies, 1992, etc.] and cutoff lows [Price and Vaughn, 1992]. Radioactive tracers and other constituents show that the downward mass flux from the stratosphere into the troposphere peaks in the spring. On the other hand, diabatic calculations show that the maximum downward mass flux takes place during the fall and winter. This discrepancy can be resolved if the seasonal variation in the tropopause height is considered. The largest exchange of mass occurs in the spring as the tropopause height moves upward toward its climatological summer position. Likewise, there is less mass exchange in the fall and winter as the tropopause moves downward [Appenezeller et al., 1996; Gettleman and Sobel, 2000; Seo and Bowman, 2002].

The lowermost stratosphere is the extratropical region between the lowest isentropic surface that is entirely within the stratosphere (~380K) and the tropopause [Hoskins, 1991; Holton et al., 1995]. The region above 380K is called the over world stratosphere. Figure 1a shows the zonal mean temperature field for January 1, 2000 with potential temperature isentropes labeled, from the U. K. Met. Office assimilation (UKMO) discussed in the next section. The figure shows that isentropes between 380K and the mid-latitude tropopause connect the tropical troposphere and the extratropical stratosphere. Thus as pointed out by Hoskins op. cit., air can move adiabatically along these isentropes both into and out of the lowermost stratosphere. Global observations of

tracer fields and potential vorticity often show rapid exchanges between the tropical upper troposphere and the lowermost stratosphere [Rood et al., 1997, Waugh and Polvani, 2000].

Radiative heating rates (Fig. 1b) show that, in the extratropical regions, there is generally net diabatic cooling along the 380K contour throughout the year [Schoeberl et al., 1998]. Thus extratropical air, once it has descended across the 380K surface into the lowermost stratosphere usually does not ascend back into the stratosphere without first entering the troposphere. As a result, almost all of the air in the stratosphere above 380K has crossed the upper tropical tropopause (above 14 km), while the air below 380K (the lowermost stratosphere) contains a mixture of air from the stratosphere and tropical troposphere air [e.g. Dessler et al., 1995; Ray et al., 1999, Dethof et al, 2000; Gettleman and Sobel, 2000; Seo and Bowman, 2002; Pfister et al. 2003].

The mass of the lowermost stratosphere is determined by the height of the tropopause and the 380K surface. If this mass were fixed, then by conservation the net transfer of material to the troposphere from the stratosphere would be equal to the mass flux across the 380K surface. However, the mass of the lowermost stratosphere fluctuates from day to day, with a general increase in the fall and decrease in the spring. In the late fall, when the stratosphere begins to cool, diabatic descent carries high potential vorticity (PV) air, ozone and trace gases downward. This descent moves the tropopause downward against tropospheric baroclinic eddy mixing which acts to reduce the vertical PV gradient [Haynes et al. 2001]. Polar stratospheric cooling also causes the 380K surface to rise. This lowering of the tropopause and the rise in the 380K surface increases the mass contained within the lowermost stratosphere.

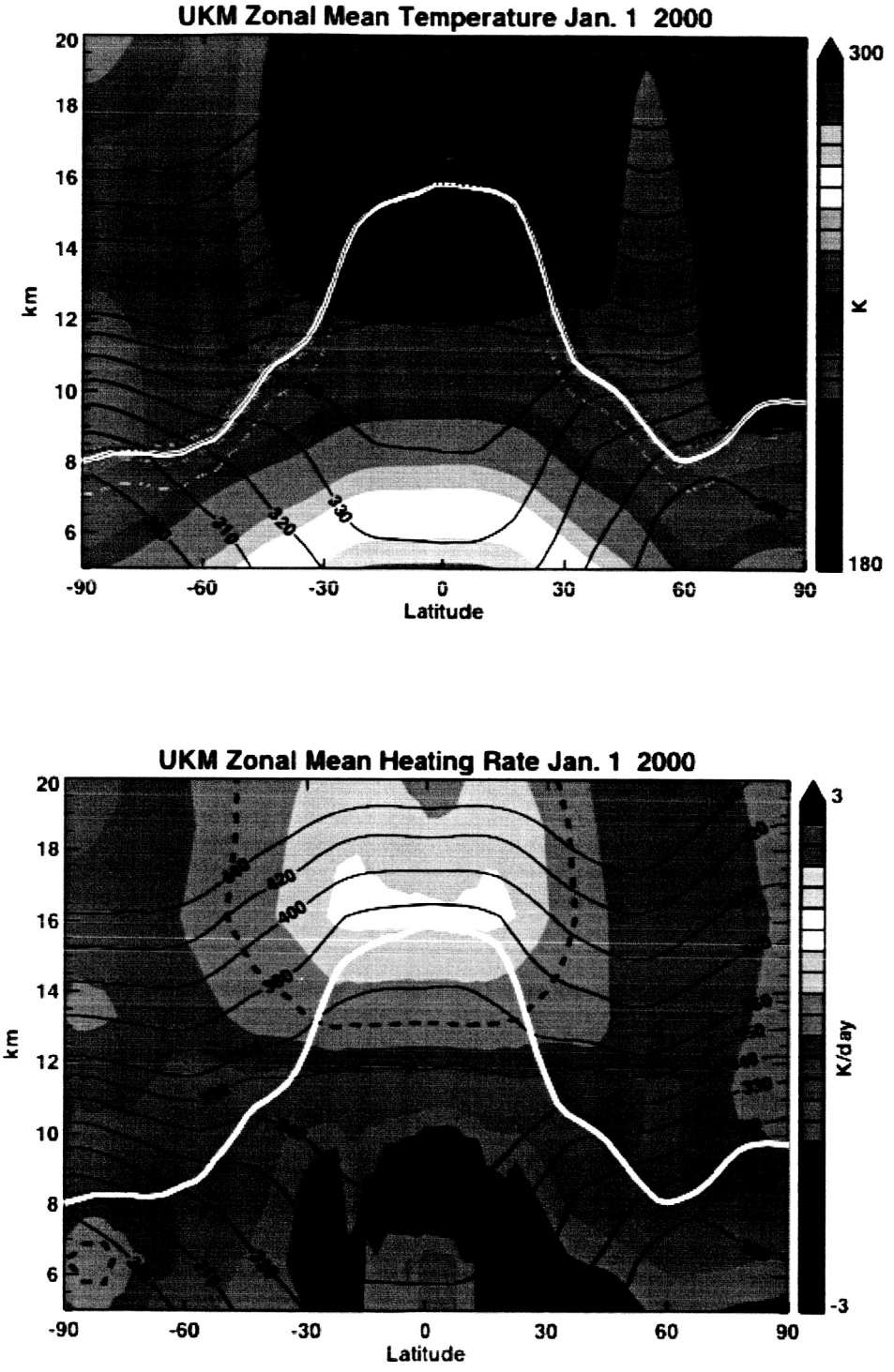

Figure 1. (Top) The zonal mean tropopause (white) from the UKMO analysis fields for Jan 1, 2000 defined by using the lower of the 3.5 PVU contour or the 2K/km lapse rate (1 PVU = 10^{-6} $Km^2s^{-1}kg^{-1}$). Zonal mean temperatures are shown in background (see color bar). Potential temperature contours are labeled in black. The orange dashed lines

indicate the zonal mean altitude of the 2, 3 and 4 PVU surfaces (lowest is 2, highest is 4). The orange solid line is the 3.5 PVU contour. The dotted line above the tropopause at middle latitudes is the WMO tropopause defined using the lapse rate of 2K/km. The lowermost stratosphere region is the surface between 380K and the tropopause. (Bottom) The zonal mean radiative heating rate in K/day. The tropopause is white. Zero heating rate contour is indicated by the dashed black line.

In the spring, the opposite occurs, with the diabatic descent weakening as the solar heating of the extratropical stratosphere increases. This causes the he tropopause to move upward and the 380K surface to move downward. The resultant mass decrease in the lowermost stratosphere flushes accumulated stratospheric trace gases into the troposphere, and this event is observed as an increase in the stratospheric abundances of trace gases in the troposphere [Monks, 2000].

How much air is transferred from the stratosphere to the troposphere in each season? Prior to the mid-1980s, attempts to estimate the amount of stratosphere-troposphere exchange focused on studying exchange events. These events appear to be dominated by "tropopause folds" where air is brought downward on the cyclonic side of the jet during the baroclinic growth phase. During the decay phase, however, the fold retracts back into the stratosphere and returns some of the stratospheric intrusion back to the stratosphere, complicating the calculation of the net exchange. Folds have been extensively studied [Danielsen and Mohnen, 1977; Shapiro, 1980] and used to estimate STE. But, counting fold-type exchange events as a method to estimate the global mass transfer is fraught with uncertainty because of the issues with net mass exchange, and since folds are often smaller than the horizontal resolution of most analyses.

Wei [1987] derived a general method for computing the mass exchange across an arbitrary surface. The exchange expression consists of two components: The first is the flux across the surface due to air mass motion; the second is the flux due to the motion of the surface itself. If the tropopause is defined as surface of PV or a tracer concentration, it is easy to see that these two components tend to oppose each other because the material surface is usually dragged along with the flow. Thus in computing the mass exchange, the Wei method consists of the evaluation the difference between two large and generally

opposing terms, and thus the net flux can be difficult to compute accurately [Wirth and Egger, 1999; Gettleman and Sobel, 2000].

Trajectory schemes evaluate the Lagrangian flux, which automatically takes into account the motion of the flow and the surface and thus avoids the difficulties of the Wei [1987] approach. Wirth and Egger [1999] computed mass exchange using a trajectory scheme and found that that approach yielded reasonable results. A trajectory scheme basically evaluates the Lagrangian flux, which automatically takes into account the motion of the flow and the surface and thus avoids the practical difficulties of the Wei [1987] scheme. Seo and Bowman [2001, 2002] and Dethof et al. [2000] have carried out Lagrangian calculations of the net mass flux across the tropopause although their approaches are quite different. Seo and Bowman [2001, 2002] performed a series of experiments releasing parcels along regular lat-long grids on either constant pressure levels or potential temperature surfaces. They assigned a mass and/or area to each of the parcels and computed the mass flux across the 2 PVU surface (1 PVU = 10^{-6} $Km^2s^{-1}kg^{-1}$) by integrating trajectories forward for one month using the UKMO analysis. They were then able to locate preferred exchange regions, estimate the mass exchange and evaluate the stratosphere to troposphere flux as well as the reverse. Month-long trajectory integrations cannot be used to produce accurate parcel positions, nor can a forward trajectory calculation be guaranteed to capture all the mass flux, but Seo and Bowman argued that because of the large number of parcels used, the results should be statistically significant. In fact, comparison of their Lagrangian technique with a Eulerian computation of the mass flux [Appenzeller et al., 1996, described below] showed good agreement. Stohl et al. [2003] discussed more detailed Lagrangian estimates of STE. Using two different trajectory models, they assessed overall mass exchange and the location of preferred regions of STE. Stohl and coworkers found that STE could be divided into two types, shallow exchange events where air has a short residence time in either the lower most stratosphere or the upper troposphere, and deep exchange events where air moves from the lower most stratosphere to deep within the troposphere. Shallow events accounted for 90% of the mass exchange Deep exchange events showed preferred occurrence along the Pacific and Atlantic storm tracks and had a strong

seasonal variation with a peak in winter. The seasonal variation and preferred location of these deep exchange events explains why the stratospheric component of tropospheric ozone shows a rapid increase in altitude [Fusco and Logan, 2003].

Dethof et al. [2000] used contour advection with surgery [Norton, 1994] to estimate the flux from the stratosphere to the troposphere and the reverse. They focused on the tropical lowermost stratosphere exchange by tracing the adiabatic evolution of tropopause contours at three different isentropic levels. They then computed the material within the contour to estimate the exchange. They found that the net adiabatic flow was from the lowermost stratosphere into the troposphere, although the fluxes in both directions were large. The main difficulty with the Dethof et al. [2000] calculation is that they focus on the exchange region between the tropics and the lowermost stratosphere stratosphere; however, adiabatic exchange can take place in regions of mid-latitude cyclogenesis and cutoff lows as well [e.g. Shapiro, 1980; Price and Vaughan, 1993].

Appenzeller et al. [1996] (hereafter A96) developed a simple Eulerian scheme to estimate STE. They noted that the net hemispheric stratosphere to troposphere mass flux is simply the difference between the time rate of change of the lowermost stratosphere mass and the amount of mass crossing the 380K surface – approximately the highest potential temperature surface that is entirely in the stratosphere. Both quantities are relatively easy to compute, given the net heating rate along the 380K surface and pressure difference between the tropopause and the 380K surface. A96 computed an annual flux of about $\sim 10^{10}$ kg/s for each hemisphere using UKMO analyses for 1992 and 1993. A96 estimated an uncertainty in their exchange rate calculation of about 20% due to differences between the net radiative heating rate estimates using different models. Stroh et al. [2003] using a kinematic Lagrangian model also estimated the mass flux. They computed a total downward mass flux of 10^{12} kg/s with an upward flux of nearly the same amount. The difference between the two $\sim 1.4 \times 10^{10}$ kg/s is the residual mass flux which is close to the net computed by A96.

The mass flux across the 380K surface is, by definition, diabatic. The flux across the tropopause can be both diabatic and adiabatic since the tropopause is not an isentropic surface (Fig. 1). The adiabatic flux takes place during the rapid exchange of air along isentropes which cross the tropopause, while the diabatic flux represents slower exchange of air across the isentropes. In the extratropics, the diabatic mass flux across the tropopause and the 380K surface is predominantly downward while the tropics the diabatic mass flux is upward. Cross-tropopause adiabatic fluxes occur in tropopause folds or as intrusions from the tropical upper troposphere into the mid-latitude lowermost stratosphere. These intrusions can transport mass in both directions. Adiabatic intrusions into the lowermost stratosphere mix with air descended from the stratosphere. It is the mixture of these two source regions that determines the chemical composition of the lowermost stratosphere.

Below, we approach the problem of determining the adiabatic and diabatic flux across the tropopause by extending the A96 technique. The method is applied to two assimilated analyses and a GCM to test the variation in the results with the analysis and the seasonal and inter annual variation of the flux. Our results, in contrast to Dethof et al. [2000] show that the net adiabatic flux must be from the troposphere into the lowermost stratosphere in order to balance the strong diabatic flux from the lowermost stratosphere into the troposphere. We also find large differences in the computed magnitude of the flux depending on the meteorological data set used.

2.0 Approach

The balance of mass in the lowermost stratosphere (M) is given by

$$\frac{dM}{dt} = F_{trop} - F_{380K} \qquad (1)$$

where F_{380K} is the diabatic flux across the 380K surface (all fluxes are positive upward). F_{trop} is the tropopause flux. A96 used (1) to estimate the tropopause flux. However, F_{trop} consists of two fluxes, the adiabatic flux (trop-a) and the diabatic flux (trop-d). Thus, if

we can compute the diabatic flux at the tropopause, the adiabatic flux can be estimated as a residual. Essentially,

$$F_{trop-a} = F_{380K} - F_{trop-d} + \frac{dM}{dt} \qquad (2)$$

for each hemisphere. The diabatic mass flux is given by $\int \dot{\theta} \frac{dp}{d\theta} dA$ where A is the area and p is pressure, θ is the potential temperature while $\dot{\theta}$ is the diabatic heating rate. We calculate the diabatic heating rates from radiative heating calculations for (see the discussion of the data sets below).

The day-to-day variations in F_{trop} are a function of the rate of change in the lowermost stratosphere mass (1) and thus dependent on the definition of the tropopause. When averaged over a year, however, we expect there to be an insignificant net change in lowermost stratosphere mass. Integrating (1) gives $\overline{F}_{380K} \approx \overline{F}_{trop}$ where the annual average is indicated by an $(\bar{})$. Since there is no dependence on M in this expression, the annual average net cross tropopause mass flux is independent of the definition of the tropopause – it is only dependent on the estimate of the 380K mass flux in each hemisphere. Since the 380K heating rate is not difficult to compute (to within 20%, A96) we expect that most estimates of the annual average mass flux for each hemisphere should approximately agree. Not surprisingly estimates of the Northern Hemisphere annual average mass flux using different tropopause definitions shown in Fig. 6 of Seo and Bowman [2002] all cluster around ~1-1.2x10^{10}kg/s.

One assumption in making the calculations using (2) is that the motion of the tropopause can be entirely described by diabatic and adiabatic motions. In practice, the tropopause is determined from a potential vorticity calculation and the height of the tropopause (and the mass of the lowermost stratosphere) may jump around as a result of the assimilation process. We also neglect the direct convective transport of mass into the extratropical

stratosphere. However, since (2) is a residual calculation, any fluxes that cannot be accounted for by the $F_{trop\text{-}d}$ calculations are assumed to be the result of an adiabatic flux.

2.1 Computation of the tropopause height

The World Meteorological Organization (WMO) defines the tropopause in terms of the temperature lapse rate ($-dT/dz$, where z is height). The tropopause is the lowest height at which the lapse rate, normally 6°-7° K/km in the troposphere, decreases to 2°K/km or less, provided that the lapse rate averaged between this height and all higher altitudes within 2 km does not exceed 2°K per km. The lapse rate tropopause (LRT) does not define any kind of conserved surface or transport barrier. However, the lapse rate tropopause nearly coincides with the location of a steep vertical gradient in the PV as might be expected from the definition of PV. In the absence of body forces or diabatic heating, PV is a conserved quantity and thus the presence of a strong PV gradient at the tropopause implies that the tropopause is a material barrier to transport. The existence of a transport barrier at the tropopause is confirmed by the existence of an ozone gradient there [e.g. Bethan, Vaughan and Reed, 1996]. Unfortunately, no standard definition for the extratropical PV tropopause exists. Holton et al. [1995] and A96 use the 2 PVU surface for the tropopause; on the other hand, Gettleman and Sobel [2000] and Dethof et al. [2000] use the 3.5 PVU surface.

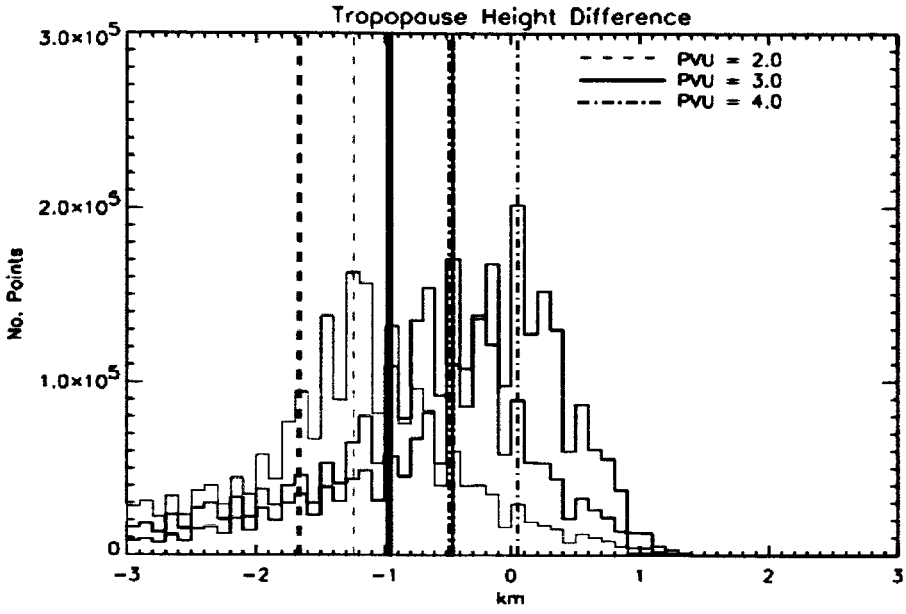

Figure 2. The height difference between the lapse rate tropopause and three PV surfaces using UKMO data (Fig.1) for the year 2000 is shown in a histogram. The thick vertical lines are the means of the distributions while the thin vertical lines are the modes.

The definition of the tropopause height is important for the computation of the day-to-day mass exchange rates and for diagnosis of the adiabatic vs. diabatic fluxes. For this study, a spline curve is fit to the gridded vertical temperature profile at each latitude-longitude grid point. Use of a spline, as opposed to linear interpolation of gridded data, allows us to estimate the location of the tropopause between the standard pressure levels. The spline grid has a 50m resolution. A number of tests were performed to optimize the spline tension to minimize overshooting and produce a reasonable fit through the gridded levels. Fig. 1 shows that the lapse rate tropopause lies above the PVU tropopause except right near the Equator. The lapse rate tropopause will also always lie at or below the cold-point tropopause (the minimum temperature altitude).

Fig. 2 shows a histogram of the distance between the LRT tropopause and three values of PVU for one year of UKMO data at all latitudes. From the histogram, the PV surface that best corresponds to the lapse rate tropopause is close to 4 PVU although the distribution is fairly broad and even 4 PVU is, on the average, below the LRT.

Historically, studies have used PV values between 3.5 and 2.0 PVU, but from Fig. 2, 2 PVU is clearly too low a value. Hoerling et al. [1991], Gettleman and Sobel [2000] and Dethof et al. [2000] used 3.5 PVU which is closer to the LRT.

In this study, the 3.5 PVU surface is used everywhere except where it exceeds the height of the LRT. If both definitions produce a tropopause above the 380K surface, we use the 380K surface as the tropopause. Figure 1 shows the location of the tropopause using the algorithm described above. The zonal mean tropopause reaches to just over 370K or about 16 km in the Tropics. Because most studies have used the 380K surface for the boundary between the lowermost stratosphere we will follow that convention although a slightly lower potential temperature value would be appropriate.

2.2 Data sets

The data sets used in this study are the UKMO assimilation [Swinbank and O'Neill, 1994], a one-year assimilation using NASA's finite-volume data assimilation system (FVDAS), and NASAs finite-volume general circulation model (FVGCM). The two NASA data sets are described by Douglass et al. [2003] and Schoeberl et al. [2003]. The FVGCM and FVDAS heating rates computed using an in-line radiative transfer model [Kiehl et al., 1998] and include latent heat release with interactive clouds. The UKMO heating rates are computed off-line using the radiative transfer model described by Rosenfield et al. [1994]; latent heat release is not included (although is probably unimportant at tropopause temperatures) and the cloud field is climatological. The use of the three different data sets should give us an idea of the uncertainty in the results.

2.3 Correction of heating rates

Integration of the net mass flux across the 380K surface using the model computed heating rates does not yield zero. This problem has been noted by previous authors, and the usual correction method is applied: the daily 380K flux residual is computed then the heating rate is adjusted by adding or subtracting a constant to produce a zero net global

flux [Rosenlof, 1995 and references therein]. This correction is only applied to the 380K surface. For surfaces below 380K, we cannot assume that the global mean mass flux is zero because of the possibility of latent, turbulent heating, and convective transport of heat exist – these are not always included in the output from the analyses. We also assume that non-radiative processes are of second order importance at the tropopause and that the bulk of the diabatic mass flux can be computed using net radiative heating rates.

3.0 Results

In the sections below we present our results. The first section illustrates the computation for a single day using the UKMO analysis.

3.1 Jan 1, 2000

The mass of the lowermost stratosphere per unit area is

$$M = (p_{trop} - p_{380K})/g \qquad (3)$$

where p_{trop} is the tropopause pressure and p_{380K} is the 380K pressure. These values are computed using the spline interpolation from meteorological gridded data sets as described above.

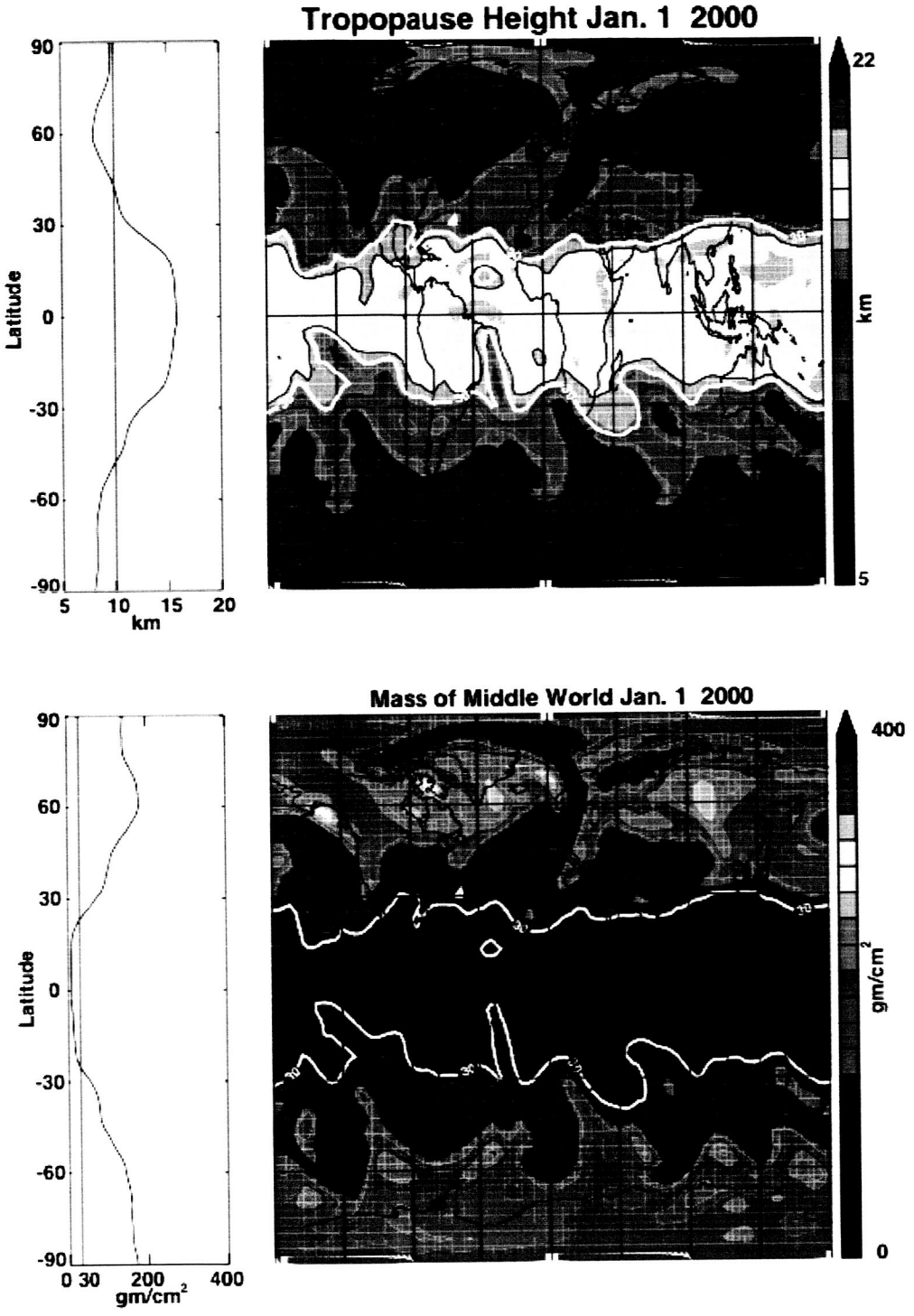

Figure 3. Top (part a), the tropopause height computed with the 3.5 PVU<LRT<380K algorithm. The bottom (part b) shows the lowermost stratosphere mass per unit area on Jan 1, 2000. The zonal mean tropopause values are shown on the left. White contour shows the 30 gm/cm^2 surface used to define the lowermost stratosphere regions in this paper.

Figure 3 shows the tropopause height and the lowermost stratosphere mass for Jan. 1, 2000. These figures show the spatial variability of the tropopause height and its strong anti-correlation to the mass of the lowermost stratosphere. Low mass regions correspond to zones with a high tropopause - such as the region extending across the Atlantic toward Europe. The west-east tilt of these systems with latitude indicates their origin in the synoptic scale weather systems that underlie them. The figures also show that the 30 gm/cm^2 mass contour does a good job defining the equatorward extent of the lowermost stratospheric region.

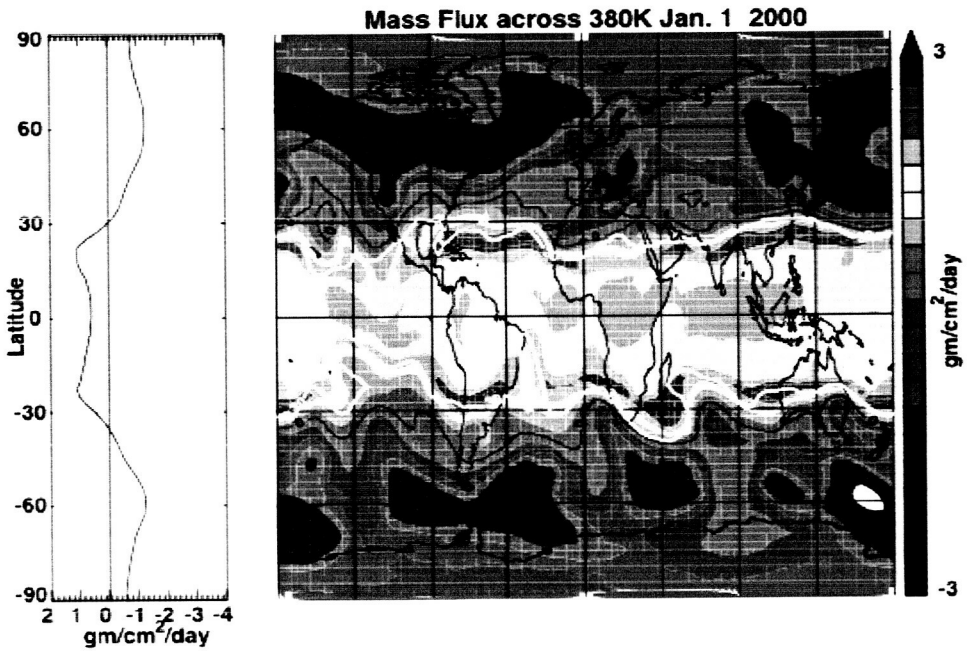

a

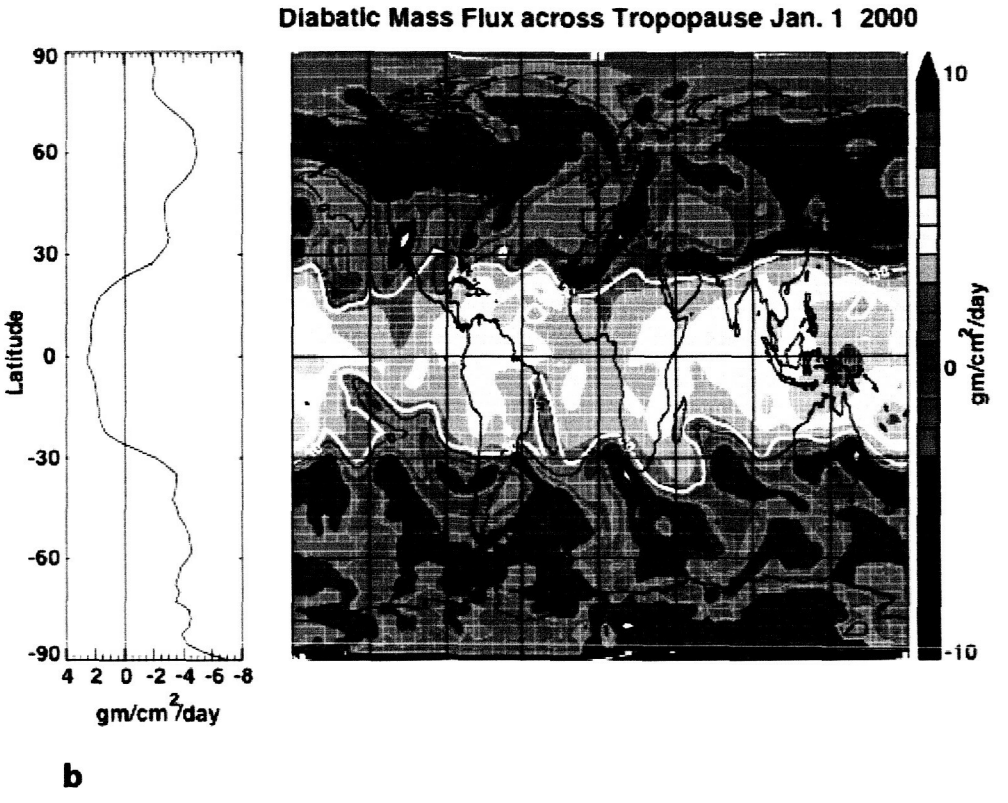

Figure 4. Top (part a), shows the diabatic mass flux across the 380K surface, and, bottom (part b)shows the diabatic mass flux across the tropopause for the same date as shown in Fig. 3. The black line shows the zero flux line separating upwelling from downwelling regions. The 30 gm/cm^2 contour from Fig. 3b is shown in white. Zonal mean values are shown on the left.

Fig. 4 shows the corresponding diabatic mass flux through the 380K surface and through the tropopause computed for Jan. 1, 2000. The 380K upwelling flux is confined generally to the tropics and the 30gm/cm^2 clearly does a reasonable job of estimating the location of the zero net-radiative-heating line. The upwelling flux shows the highest values near the northern and southern edges of the upwelling zone. This edge enhancement is absent in the tropical heating rates (not shown) and is due to the increase in atmospheric mass as the 380K surface starts to descend toward the extra-tropics. Within the tropics, there is a smaller upward flux at 380K than at the tropopause (see zonal mean values in Fig. 4) which is expected since the tropopause computed here is closer to the higher mass 370K surface. Since our computations, following A96, compute the net downwelling flux at the

380K surface, we note that the difference in mass flux across the 370K and 380 K surfaces means that some upwelling mass is diverted into the extratropical stratosphere from the tropical gap between 370K and 380K.. This diverted flux is roughly twice as large as the 380K flux and because the isentropes are fairly flat in this region, the flux is adiabatic. We will return to this point in the discussion of the overall results below.

From Figure 4b we see that the tropopause upward mass flux is highest over the Indonesian region where the tropopause is coldest. The mid latitude downwelling flux is also weakest in regions with a high, cold tropopause. We expect weaker extratropical cooling rates where the tropopause is high since a high tropopause is colder and closer to radiative equilibrium (see Fig. 1b).

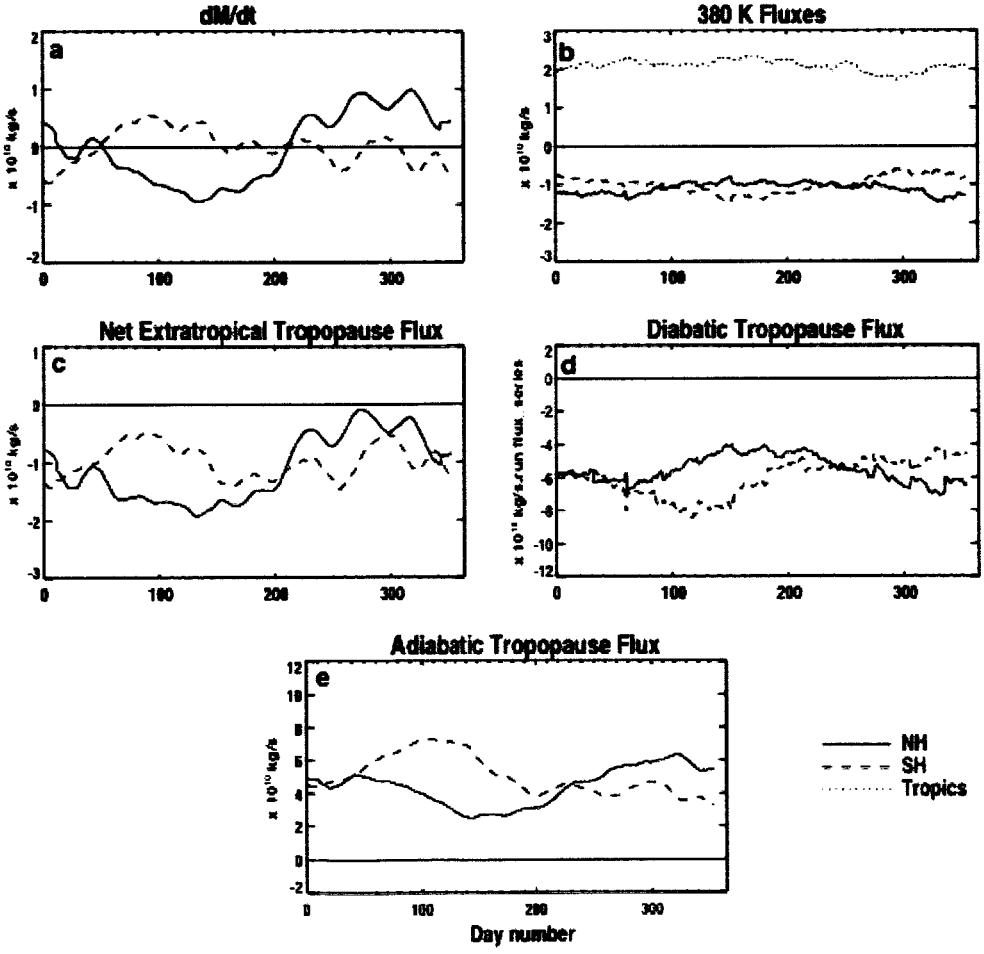

Figure 5. Time series of UKMO mass changes and mass fluxes for the year 2000. Upper left (a), the time rate of change in the lowermost stratosphere mass for the Northern and Southern hemisphere. Upper right (b), the 380K mass fluxes. Center left (c), F_{trop}, the net tropopause mass flux obtained by subtracting the lowermost stratosphere mass change from the 380K downwelling flux (A96). Center right (d), the net diabatic mass flux at the tropopause computed from the net tropopause heating rates. Bottom (e), the adiabatic flux computed from the difference between the diabatic flux and the net flux. Solid line – Northern Hemisphere downwelling (NH), dashed line- Southern Hemisphere (SH), dotted line-tropical upwelling. Units are 10^{10} kg/s

3.2 The annual flux cycle

To use Eq. (2), we compute the daily mass of the lowermost stratosphere for each hemisphere (where the lowermost stratosphere mass is greater than 30 gm/cm^2 (Fig. 3)), the 380K flux, and the tropopause diabatic flux.. The net extratropical tropopause flux (F_{trop}) is computed following A96 using the lowermost stratosphere mass tendency and the diabatic 380K flux (Eq. 1). The tropopause adiabatic flux is ($F_{trop\text{-}a}$) estimated using the difference between the diabatic fluxes ($F_{trop\text{-}d}$) and the net tropopause flux (F_{trop}) (Eq. 2). The fluxes are computed for each day. The daily lowermost stratosphere mass is smoothed with a 20 day box-car filter and then the time derivative is computed. The diabatic fluxes are also smoothed with the same filter.

Figure 5 shows the annual time series of lowermost stratosphere mass tendency and mass fluxes computed using the UKMO data, the annual averaged fluxes are listed in Table 1 below. The flux variations in Fig. 5 are in good agreement with A96, who found that the net extratropical mass flux is largest in late winter/spring and weaker in later summer/fall for both hemispheres. Since the changes in the 380K mass fluxes are relatively small throughout the annual cycle, the variations in the net flux are almost entirely driven by the change in the lowermost stratospheric mass which begins to decrease in February (the tendency is negative and growing). The

lowermost stratosphere region reaches a minimum mass in mid-July. Then the mass then begins to increase rapidly with the onset of northern winter. The southern hemisphere lowermost stratosphere mirrors these changes with a six month phase shift and about half the amplitude. However, there is no strong spring decrease in the southern hemisphere lowermost stratosphere mass.

The UKMO extratropical diabatic tropopause flux ($F_{trop\text{-}d}$) is shown in Fig. 5. The diabatic flux follows the changes in the tropopause mean temperature. In the UKMO assimilation the mean temperature rises to 225K in the summer and falls in the winter to 218K for both hemispheres. The fact that $F_{trop\text{-}d}$ always exceeds the net tropopause flux (F_{trop}) means that air is always flowing adiabatically into the lowermost stratosphere from the troposphere ($F_{trop\text{-}a}$ is positive). We also note that the average adiabatic flux is ~ 6x 10^{10} kg/s, much larger than the tropical upwelling flux of ~ 2x 10^{10} kg/s. This means that three times more air is entering the lowermost stratosphere adiabatically through tropical-extratropical tropopause than by ascending diabatically through the tropical tropopause and then descending across the 380K surface into the extratropical lowermost stratosphere.

Our calculation of large annually persistent net adiabatic flux of air into the lowermost stratosphere is in contrast to the results of Dethof et al. [2000]. We note again that Dethof et al. made a direct estimate of the adiabatic exchange focusing on the tropical-subtropical lowermost stratosphere region where the tropopause changes altitude rapidly. Evaluating the net exchange through contour advection calculations is difficult since transfer of material between the lowermost stratosphere and the tropical upper troposphere is characterized by large exchange events – thus this method is equivalent to quantifying the number and magnitude of such events. Second, adiabatic exchange can occur wherever the tropopause crosses isentropic surfaces (such as regions of rapid folding) and neglect of mid-latitude exchange through folding will result in an underestimate of the adiabatic exchange rate. Seo and Bowman [2002] draw the same conclusion as we do noting that estimates of

downward mass flux, where tropopause folding is accounted for are much higher than that estimated by Dethof et al. [2000].

3.4 Comparison between three data sets

It is useful to check to see if the UKMO estimate for the size and sign of the adiabatic mass flux holds for other data sets. Our flux analysis has been performed using the year of FVDAS analysis as well as several years of FVGCM output. Note that the FVGCM output does not correspond to any particular observational year.

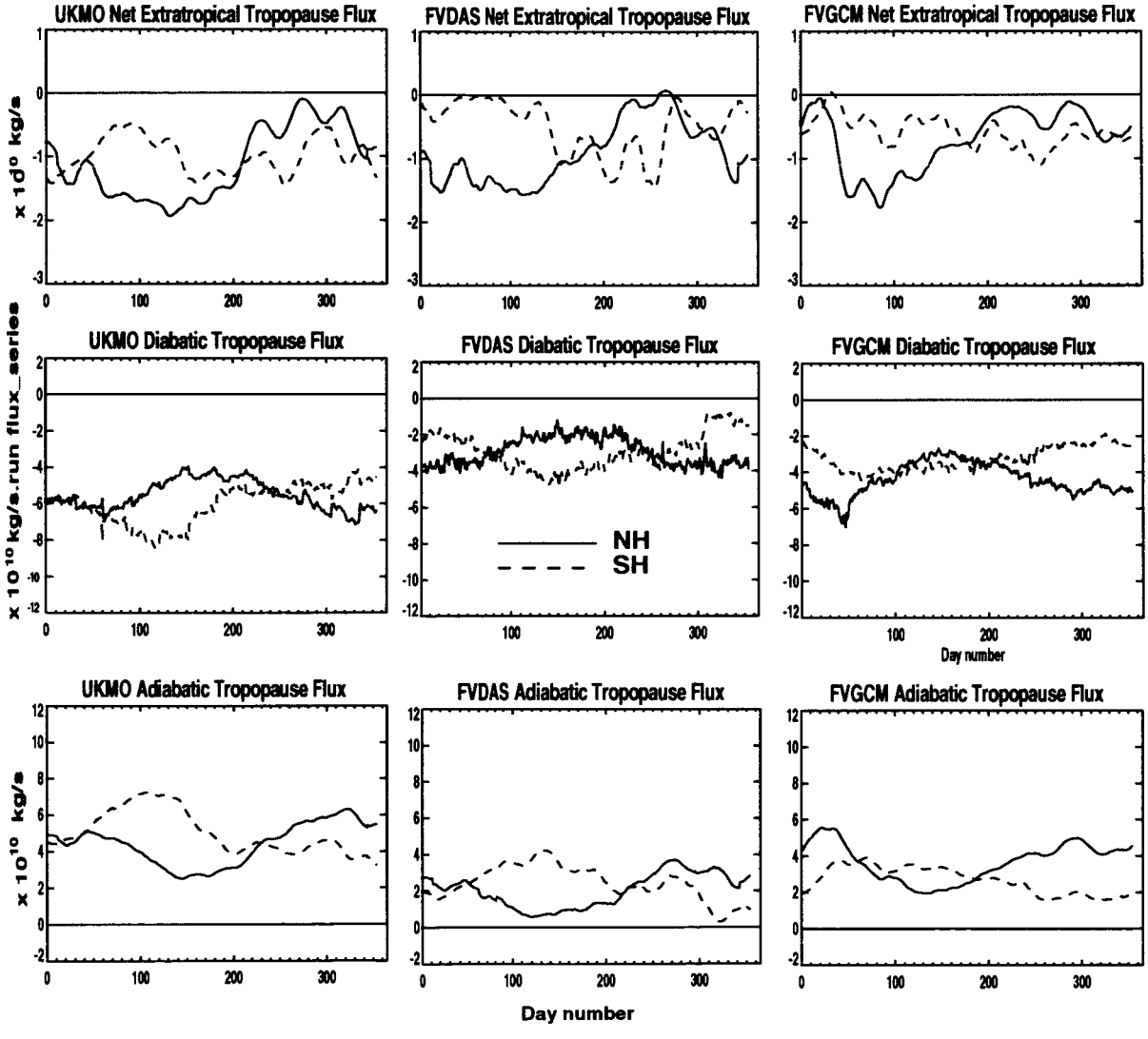

Figure 6. The net, diabatic and adiabatic flux time series for three data sets: left, UKMO, middle FVGCMS, right FVDAS. The DAS sets (left and right) are for the year 2000. The middle data set is from one year of the GCM used as the core of the FVDAS – it does not correspond to any actual year.

Figure 6 compares the annual cycle in the three data sets. The overall shape of the net flux, diabatic and adiabatic flux annual cycle are similar. The two assimilation data sets also generally agree on the overall value of the net tropopause flux in the northern hemisphere, but there is less agreement on the southern hemisphere values. The main difference between the FVDAS and the UKMO appears to be an offset in the diabatic flux of about ~3 x 10^{10} kg/sec. The FVGCM shows slightly less of an offset. The adiabatic fluxes, computed as a residual reflect the differences in the diabatic fluxes, but the analyses are consistent in that the adiabatic flow is from the upper tropical tropopause into the lowermost stratosphere.

Table 1 shows the annual average fluxes and compares our results to previous studies. The studies shown tend to agree on the magnitude of the average F_{trop} as ~ 10^{10} kg/s. This is not surprising based upon the discussion in Section 2 where we noted that annual averaged net flux is not dependent on the definition of the tropopause height. The 20% differences between analyses are probably due to differences in radiation schemes and interannual variability (as will be shown in Figure 9 below). The Table also shows that the UKMO diabatic fluxes are nearly twice as large as the FVGCM and FVDAS fluxes.

Table 1. Annual average tropopause fluxes of mass for three data sets compared with other estimates. The years used in the calculations and data set are indicated below the reference. ECMWF is the European Center for Medium Range Forecasting reanalysis; GEOS-3 is an assimilation data set that preceded FVDAS [see Douglass et al. 2003]. Fluxes are all extra-tropical except as indicated.

Annual Average Fluxes x 10^{10} kg/s	UKMO 2000	FVDAS 2000	FVGCM	A96 1992-3 UKMO	Seo & Bowman [2002] 1996-7 UKMO	Dethof et al. [2000] 1997-8 ECMWF	Gettleman & Sobel [2000] 1995-98 GEOS-3	Stroh et al. [2003] ECMWF
Tropical Upwelling (380K)	2.1	1.5	1.3	2.1				
Net Flux (F_{trop}) SH	-1.0	-0.5	-0.58	-1.0				
Net Flux (F_{trop}) NH	-1.1	-0.9	-0.72	~1.1	~1.2		~1.2	-1.4
Diabatic Flux ($F_{trop\text{-}d}$) SH	-6.0	-3	-3.2					
Diabatic Flux ($F_{trop\text{-}d}$) NH	-5.5	-2.9	-4.4					
Adiabatic Flux ($F_{trop\text{-}a}$) SH	5.1	2.5	2.7					
Adiabatic Flux ($F_{trop\text{-}a}$) NH	4.4	2.0	3.7			~ -0.4		

3.5 The differences between the tropopause diabatic mass fluxes between data sets

The diabatic tropopause fluxes are computed from the net heating rates. Figure 7a shows a comparison of the tropopause heating rates relative to the UKMO data assimilation for 10 days in January 2000. Tests with other periods show the same

bias. At extratropical latitudes (where there is net cooling), the UKMO cooling rate is up to 0.8 K/day greater than either the FVDAS or the FVGCM. At tropical latitudes, where there is heating (see Fig. 1) the bias is opposite with UKMO showing 0.3 K/day less heating. These biases arise mostly from a tropopause temperature differences as illustrated in Figure 7c. This connection to the heating rates occurs, to first order, because when the extratropical tropopause temperatures are colder, the region is then closer to radiative equilibrium and the cooling rates are smaller. The presence of clouds in the heating rate computation is also important. For UKMO heating rates, a cloud climatology is used, whereas the FVDAS and FVGCM have interactive cloud fields. Thus we do not expect the heating rate biases to be totally due to tropopause temperature differences.

The tropopause temperature differences can be partly explained by differences in the tropopause height estimate (Fig. 7b). For extratropical tropopause heights, (6-10 km), the pattern of height biases is similar to the temperature biases. A height bias of one km could approximately explain a ~7K bias in temperature (using the average lapse rate). Thus the height bias can account for most of the temperature differences see in Fig. 7c. In passing we note that the FVGCM is the most cold biased.

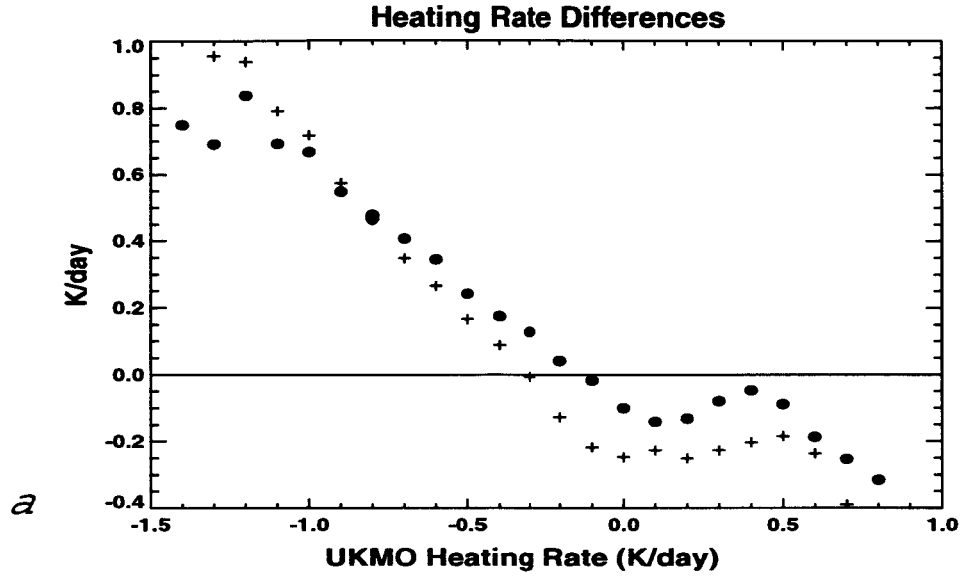
Heating Rate Differences
K/day
UKMO Heating Rate (K/day)

a

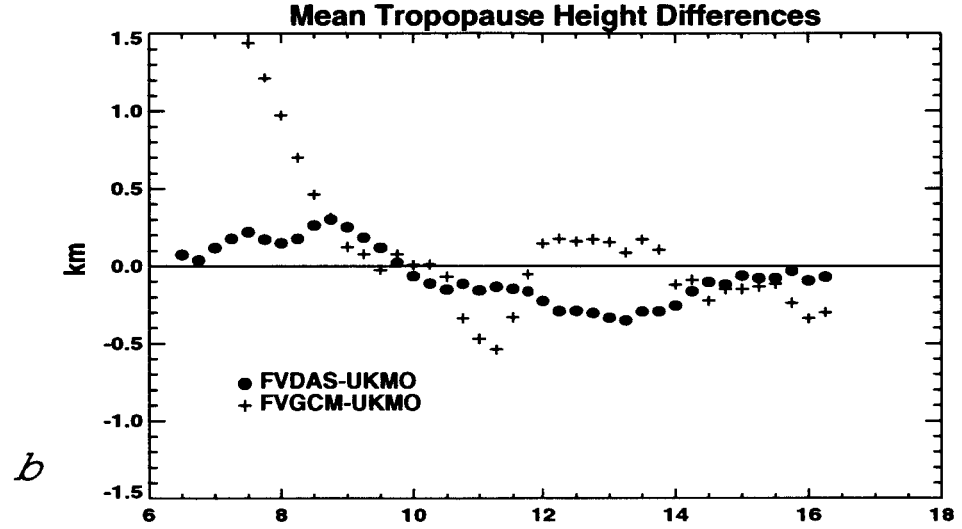
Mean Tropopause Height Differences
km
FVDAS-UKMO
FVGCM-UKMO
UKMO Height

b

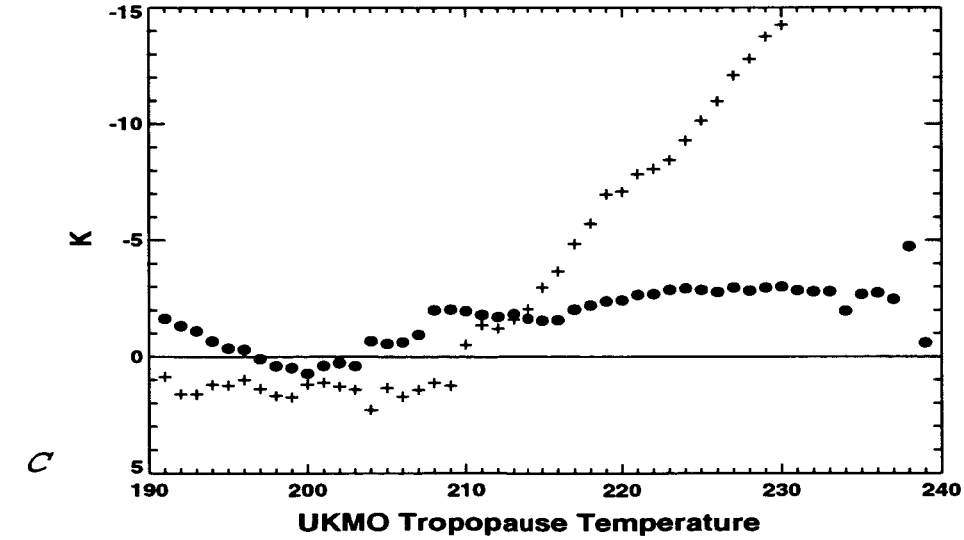
Mean Tropopause Temperature Differences
K
UKMO Tropopause Temperature

c

Figure 7. Top (part a) comparison of tropopause heating rates relative to the UKMO heating rate. Middle (part b), comparison of tropopause height differences as a function of height. Bottom (part c) comparison of tropopause temperature difference as a function of temperature. The right side of (part a) (heating) corresponds to the tropics, the left side (cooling), extra tropics. The left side of part b corresponds to the extra-tropics, the right side, tropics. The left side of part c corresponds to thetropics, the right side, extra-tropics. In the figures the data are interpolated onto the UKMO grid and the differences are binned into the intervals shown. Data bins with less than 5 data points are not plotted. Data is from Jan 1-5 for the data sets shown in Figure 6.

The comparison shown in Fig. 7 does not answer the question: Which assimilation more accurately represents the measured tropopause temperature and therefore gives the best estimate of the flux? To answer this question we compare radiosonde estimates of the tropopause temperatures to the assimilation. The assimilation systems already use the radiosonde information, but the differences between assimilation estimates of tropopause temperature (Fig. 7c) suggest that the UKMO and FVDAS may be using (or weighting) the information in different ways. To estimate the radiosonde tropopause height we estimate the altitude of the LRT using the spline method described above. The data are further filtered by eliminating sonde tropopause estimates that differ by more than 2 km from UKMO DAS tropopause. Because there are fewer sondes than assimilation grid points, we have processed two months of observations (Jan. and Feb. 2000) to build up the statistics. Thus there will be differences in results shown Fig. 7 compared to our results shown in Fig. 8. The sonde LRT was compared to DAS LRT and DAS PV tropopause. The results, shown in Figure 8, were nearly identical.

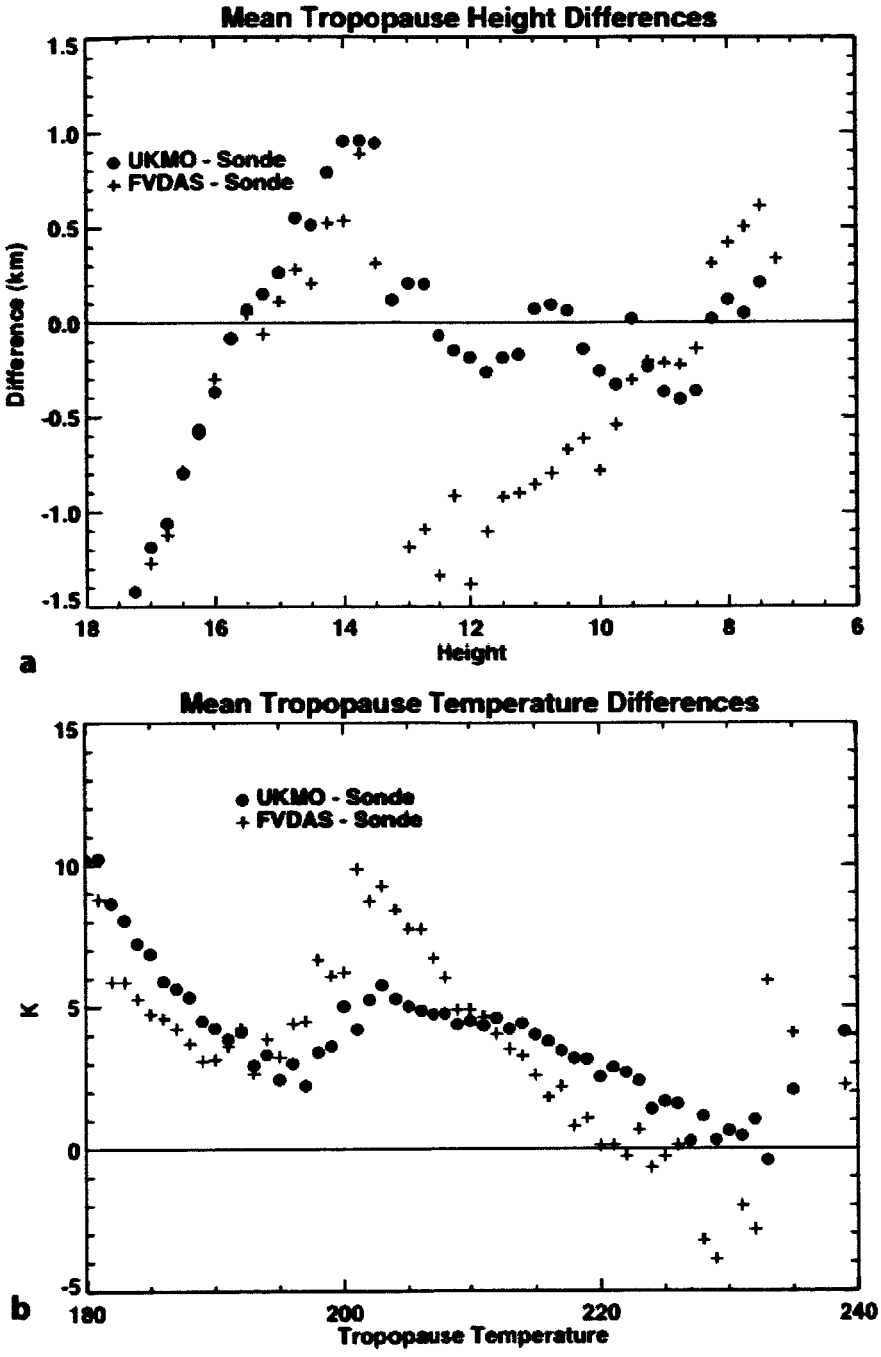

Figure 8. The difference between sonde tropopause heights (part a) and temperatures (part b) as a function of data assimilation tropopause temperature and heights, respectively, as in Fig. 7. Data is for month of January-February 2000.

From Fig. 8a, the UKMO extra-tropical tropopause is up to ~0.5 km lower than the sonde tropopause, roughly independent of the tropopause height. This extratropical height displacement would produce a warm bias for the assimilation data sets of up to 3-4 K (assuming the 7 K/km lapse rate) compared to the sondes. Figure 8b shows that there is in fact an extra-tropical warm bias of about this magnitude. The FVDAS extratropical tropopause height bias appears to decrease as the tropopause heights are lower. But the FVDAS height bias is larger at mid-latitudes as is the warm temperature bias. The warm tropopause bias reflects the sonde height bias pattern to some extent, although the height bias doesn't completely explain the temperature bias.

Because the extra-tropical diabatic mass flux is controlled by the tropopause temperature, the radiosonde comparisons suggest that our diabatic tropopause flux estimate would be too high because our DAS tropopause is too warm. In other words, since the assimilation tropopause temperatures are warmer than radiosonde tropopause temperatures, our estimates of the diabatic mass flux will be an upper limit.

The opposite effect occurs in the tropics. Comparing the tropical sonde temperatures and the model temperatures in Fig. 8b, the sondes are ~5° K colder than the assimilated data. With a colder tropopause the upwelling flux will be larger (net diabatic heating will increase). By correlating the assimilated temperature and the computed heating rate at the tropical tropopause, the Newtonian cooling coefficient is computed to be ~0.03 $days^{-1}$. Since our computed tropical tropopause heating rate is about 0.6 K/day (Fig. 7a), for a ~5 K colder tropopause, the heating would increase by 0.15 K/day or a roughly 25%. The tropical tropopause upward mass flux would increase by the same percent as would the downward mid-latitude flux. The mid-latitude and tropical corrections to the tropopause temperatures would reduce our adiabatic flux estimates.

3.7 Interannual variability in mass exchange

Is the year 2000 anomalous with regard to flux estimates? Fig. 9 shows the interannual variability of the annual average mass fluxes and tropopause temperatures for the three

data sets. The net tropopause mass flux shows small relative differences between the data sets, about ~20% year-to-year variability. The diabatic and adiabatic fluxes show much smaller variability than the variability between the data sets as seen in Table 1 and discussed above. As discussed in the last section this variability is shows up in the tropopause temperatures as seen in Fig 9b

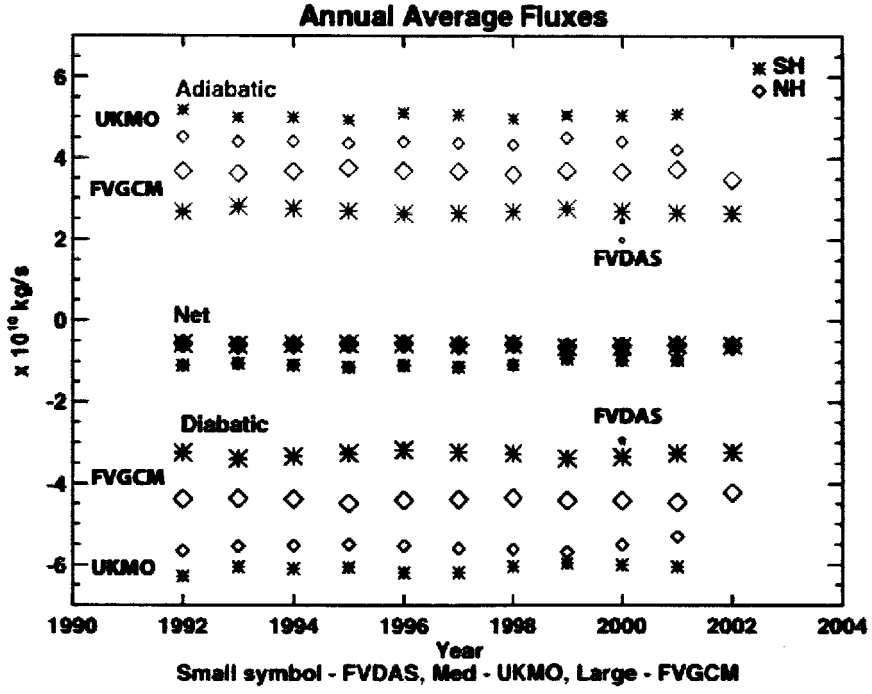

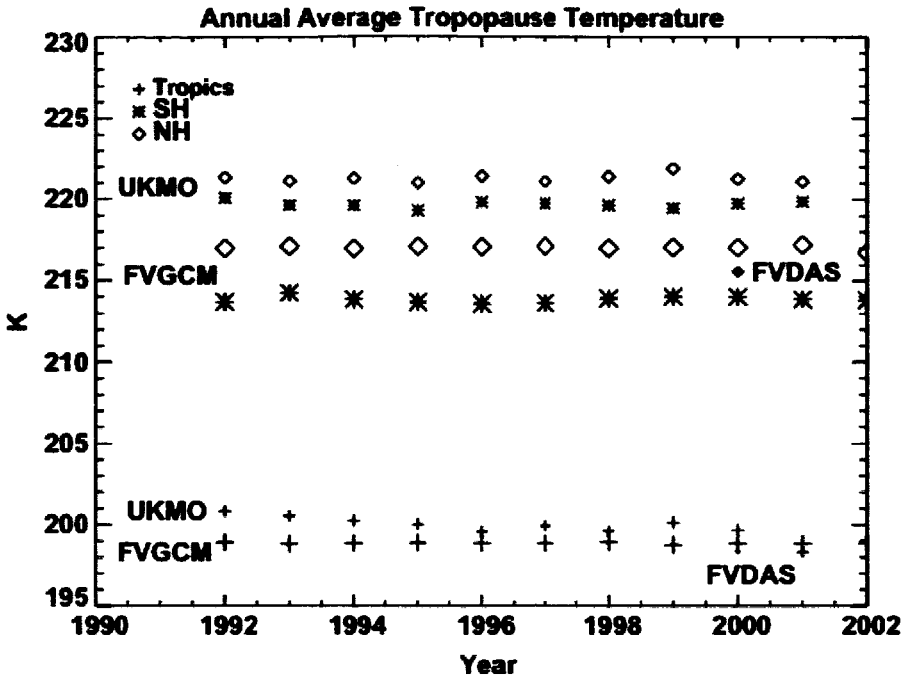

Figure 9 Top (part a), annual mean net (red), adiabatic (green) and diabatic (purple) mass fluxes from the FVGCM, UKMO and FVDAS. Bottom (part b), the annual mean tropopause temperatures from the three data sets. Symbol size denotes the data set, Color in the top figure distinguishes net, diabatic and the residual adiabatic flux.

4.0 Summary and discussion

The global net mass flux from the stratosphere to the troposphere was computed using the A96 technique for three data sets, UKMO, FVDAS and FVGCM, the first two being assimilation analyses. These data sets generally agree on the NH annual average net downward mass flux of ~10^{10} Kg/s, and this value is consistent with other modern estimates (Table 1). The annually averaged mass flux is not dependent on the definition of the tropopause but is only dependent on the flux through the 380K surface. Despite this general agreement, there is as much as a 20% difference in the NH net mass flux between the two assimilation data sets used here. The estimate of the SH annual average net downward mass flux shows a 50% difference between data sets. The variation of the net flux throughout the year shows the rapid Northern Hemisphere decrease of the

lowermost stratosphere mass in the spring and a build up in the fall. This cycle is much weaker in the southern hemisphere.

The diabatic mass flux follows an annual cycle that follows the tropopause temperature, peaking in summer and minimizing in winter. This mass flux is five to six times larger than the net tropopause mass flux. Because there is so much mass crossing the tropopause relative to the mass crossing the 380K surface, there must be an infusion of mass from the tropical upper troposphere into the lowermost stratosphere. This mass must be moving adiabatically across isentropes that intersect both regions. Fig. 10 shows a cartoon illustration of these annually averaged mass fluxes computed for ten years of UKMO assimilation and the year of FVDAS. The figure is overlaid on the zonal mean isentropes shown in Fig. 1.

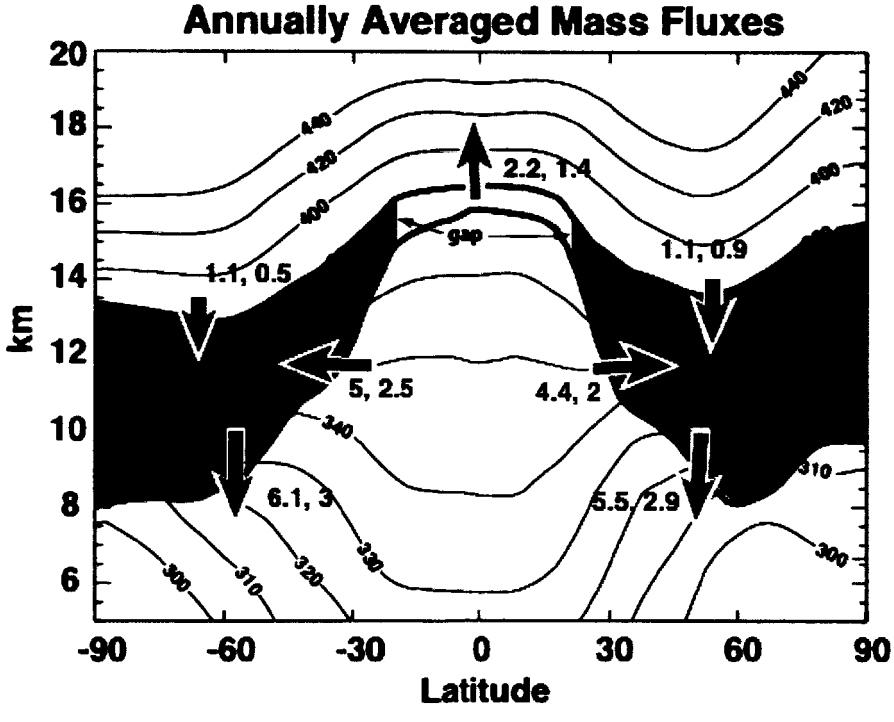

Figure 10. Cartoon illustration of the annually averaged mass fluxes from 1992-2001 for the UKMO data set (red) and the FVDAS (blue). Adiabatic fluxes are shown in black, diabatic fluxes are shown in green. Numbers in red are the fluxes in kg/sec while numbers in black indicate the potential temperature of the contours shown. Blue areas indicate the NH and SH lowermost stratosphere. The dark blue line shows the tropopause

while the red line is the 380K contour. The tropical gap between the tropopause and the 380 K surface is indicated in the figure.

The implication that there must be a large adiabatic mass flux into the lowermost stratosphere is contrary to the computations by Dethof et al. [2000] but consistent with Seo and Bowman [2001]. As an aside, about 20% of this adiabatic flux occurs as a result of the difference between the 380K tropical upwelling flux calculations and the tropical tropopause upwelling flux (closer to 370K) which is evident if we compare the tropical upwelling mass flux between Figs 4a and 4b. This is the flux that occurs in the tropical-extratropical "gap" between the tropopause and 380K seen in Fig. 10.

Our analysis is somewhat different from the calculations of Stroh et al. [2003]. Like Seo and Bowman [2001] they used a Lagrangian model, but performed kinematic trajectory calculations. Kinematic trajectories use the omega field from the analyses and cannot be used to partition the flow into adiabatic and diabatic components. As a result of of noise-like pressure variations due aliased adiabatic flows (such as high frequency gravity waves), kinematic methods can overestimate shallow exchange of mass near the tropopause. Stroh et al. [2003] Northern Hemisphere annually averaged total mass exchange from the stratosphere to the troposphere is ~1.3 $x10^{12}$ kg/s which ~20 times larger than the diabatic flux computed here. Of this total mass exchange, they estimate that about 10% is deep involving large changes in parcel potential temperature. If we assume that all the deep exchange is equivalent to our diabatic flux, then the Stroh et al. estimate of the diabatic flux would be about 13 $x10^{10}$ kg/s which is within a factor of 2-4 of estimates from the models (Table 1). This is probably reasonable agreement considering the different approaches.

The adiabatic flux into the lower most stratosphere, dilutes air descending across the 380K surface from higher stratosphere. This dilution process is manifested in the strong north-south transport events as seen in Figure 3 and as has been noted by Dethof et al. [2000].

The differences in diabatic fluxes between the assimilation data sets are much larger than interannual variability and are related to the differences in tropopause temperatures and heights. The extratropical UKMO tropopause diabatic mass flux is larger than FVDAS because the extratropical cooling rates are larger. This is because UKMO tropopause is warm biased and lower in altitude than FVDAS. Comparison to extratropical radiosondes tropopause temperatures and heights show that both assimilation data sets are warm biased and this is consistent with a lower assignment of the tropopause height in the DAS.

The disagreement in mass fluxes between the two assimilation data sets suggests that there will be a disagreement in tracer fluxes as well. This disagreement can strongly affect model estimates of the lowermost stratosphere composition and composition change as a result of climate change. The large infusion of mass from the upper tropical troposphere into the lowermost stratosphere may also affect ozone loss since short-lived chlorine halocarbon substitutes will be carried into the lower stratosphere through this path.

Acknowledgements

The author is indebted to Steven Pawson, Anne Douglass, Andy Dessler and Mark Olsen for helpful discussions.

5. References

Appenzeller, C. J., and H. C. Davies, Structure of stratospheric intrusions into the troposphere, Nature, 358, 570-572. 1992.

Appenzeller, C., J. R. Holton and K. Rosenlof, Seasonal variation of mass transport across the tropopause, J. Geophys. Res., 101, 15071-15078, 1996.

Bethan, S., G. Vaughan and S. Reed, A comparison of ozone and thermal tropopause heights and the impact of tropopause definition on quantifying the ozone content of the tropopause, Q. J. R. Met. Soc., 929-944, 1966.

Danielsen, E. F. Stratosphere-troposphere exchange based upon radioactivity, ozone and potential vorticity, J. Atmos. Sci, 25, 502-518, 1968.

Danielsen, E. F. and V. A. Mohnen, Project Dustorm report: Ozone transport, in situ measurements, and meteorological analyses of tropopause folding, J. Geophys, Res. 82, 5867-5877, 1977.

Dessler et al., Mechanisms controlling water vapor in the lower stratosphere: "A tale of two stratospheres", JGR, 100, 23,167-23,172, 1995.

Dethof, A., A. O'Neill and J. Slingo, Quantification of the isentropic mass transport across the dynamical tropopause, J. Geophys. Res., 105, 12,279-12,293, 2000.

Douglass, A. R., M. R. Schoeberl, R. B Rood and S. Pawson, Evaluation of transport in the lower tropical stratosphere in a global chemistry and transport model. J. Geophys. Res., 108, doi:10.1029/2002JD002696, 2003.

Fusco, A. C., and J. A. Logan, Analysis of the 1970-1995 trends in tropospheric ozone at Northern Hemisphere midlatitudes with the GEOS-CHEM model. J. Geophys. Res., 108, 4449, doi: 10.1029/2002JD002525.

Gettleman A. and A. H. Sobel, Direct diagnoses of stratosphere-troposphere exchange, J. Atmos. Sci., 57, 3-16, 2000.

Haynes, P. H., J. Scinocca, M. Greenslade. Formation and maintenance of the extratropical tropopause by baroclinic eddies, Geophys Res Lett, 28, 4,179-4,182, 2001.

Hoerling, M. P., T. K. Schaack and A. J. Lenzen, Global objective tropopause analysis, Mon.Wea. Rev., 119, 1816-1831, 1991.

Hoerling, M. P., T. K. Schaack and A. J. Lenzen, A global analysis of stratospheric-tropospheric exchange during northern winter, Mon.Wea. Rev., 121, 162-172, 1993.

Holton, J. R., P. H. Haynes, M. E. McIntyre A. R. Douglass, R. B. Rood, and L. Pfister, Stratosphere-Troposphere exchange, Reviews of Geophys., *33,* 403-439, 1995.

Hoskins, B. J., Toward a PV-theta view of the general circulation, Tellus, 43AB, 27-35, 1991

Kiehl, J. T., J. J. Hack, G. B. Bonan, B. A. Boville, D. L. Williamson, and P. J. Rasch, The National Center for Atmospheric Research Community Climate Model: CCM3, J. Climate, 11, 1131-1149, 1998.

Monks, P. S., A review of the observations and ortings of the spring ozone maximum, Atmos. Eniviron., 3, 3545-3561, 2000.

Norton, W. A., Breaking Rossby waves in a model stratosphere diagnosed by a vortex following coordinate system and a technique for advecting material contours, J. Atmos. Sci., 51, 654-673, 1994.

Olsen, M. A., A. R. Douglass, and M. R. Schoeberl, Estimating the downward cross-tropopause ozone flux using column ozone and potential vorticity, J. Geophys. Res., 107, doi:10.1029/2001JD002041, 2002.

Pfister, L. et al., Processes controlling water vapor in the winter Arctic tropopause region, J. Geophys. Res., 108, doi:10.1029/2001JD001067, 2003.

Price, J. D. and G. Vaughan, The potential for stratospher troposphere exchange in cutoff low systems, Q. J. R. Met Soc., 119, 343-365, 1993.

Ray, E. A., et al., Transport into the northern hemisphere lowermost stratosphere revealed by in situ tracer measurements, J. Geophys. Res., 104, 26,565-26,580, 1999.

Rood, R. B., A. R. Douglass, M. C. Cerniglia, W. G. Read, Synoptic scale mass exhange from the troposphere to the stratosphere, J. Geophys. Res., 102, 23467-23486, 1997.

Rosenfield, J. E., P. A. Newman, M. R. Schoeberl, Computations of Diabatic Descent in the Stratospheric Polar Vortex, J. Geophys. Res., 99, 16,677-16,689, 1994.

Rosenlof, K. H. , and J. R. Holton, Estimates of the stratospheric residual circulation using the downward control pronciple, J. Geophys. Res., 98, 10465-10479, 1993.

Rosenlof, K. H., The seasonal cycle of the residual mean meridional circulation in the stratosphere, J. Geophys. Res. 100, 5173-5191, 1995.

Schoeberl, M. R., C. Jackman, and J. Rosenfield, A Lagrangian Estimate of aircraft effluent lifetime, J. Geophys. Res., 103,10817-10825, 1998.

Schoeberl, M. R., A. R. Douglass, Z. Zhu and S. Pawson, A comparison of the lower stratospheric age spectra derived from a general cirulatio model and two data assimilation systems, J. Geophys. Res. 108, 4113, doi:`0.`029/2002JD002652, 2003.

Seo, K-H and K. Bowman, Lagrangian estimate of global stratosphere-troposphere mass exchange, J. Geophys. Res., 107, doi:10.1029/2002JD002441, 2002.

Seo, K-H and K. Bowman, Climatology of isentropic cross-tropopause exchange, J. Geophys. Res.,106,28159-28172, 2001.

Shapiro, M. A., Turbulent mixing within tropopause folds as a mechanism for the exchange of chemical constituents between the stratosphere and troposphere, J. Atmos. Sci., 37, 994-1004, 1980.

Staley, D. O., On the mechanism of mass and radioactivity transport from the stratosphere to the troposphere, J. Atmos. Sci., 19, 450-467, 1962.

Stroh, A. et al., A new perspective on stratosphere-troposphere exchange, Bull. Amer. Meteor. Soc., 84, 1565-1573, 2003.

Swinbank, R. and A. O'Neill, A stratosphere-troposphere data assimilation system, Mon. Weather Rev., 122, 686-702, 1994.

Waugh, D. W. and L. M. Polvani, Climatology of intrusions into the tropical upper troposphere, Geophys, Res. Lett., 27, 3857-3860, 2000.

Wei, M. Y., A new formulation of the exchange of mass and trace constituents between the stratosphere and the troposphere, J. Atmos. Sci., 44, 3079-3086, 1987.

Wirth, V. and J. Egger, Diagnosing extratropical synoptic-scale stratosphere-troposphere exchange: A case study. Quart. J. Roy. Met. Soc. 125, 635-655, 1999.